Journal of Chromatography A, 1218 (2011) 4452–4461

Contents lists available at ScienceDirect

Journal of Chromatography A

journal homepage: www.elsevier.com/locate/chroma

Accurate measurements of peak variances: Importance of this accuracy in the determination of the true corrected plate heights of chromatographic columns

Fabrice Gritti, Georges Guiochon*

Department of Chemistry, University of Tennessee, Knoxville, TN 37996-1600, USA

ARTICLE INFO

Article history:
Received 22 September 2010
Received in revised form 24 January 2011
Accepted 10 May 2011
Available online 19 May 2011

Keywords:
Column efficiency
Peak moments
Accuracy
Precision
HETP
Uracil
Naphthalene

ABSTRACT

The true efficiency of a column is derived from the differences between the variances of the peak profiles of the same compound recorded in the presence and the absence of the chromatographic column. These variances are usually derived using one of three methods: (1) the retention time of the peak apex and its half-height width; (2) the moments of the best fit between the experimental data and a hybrid response function, e.g., an exponentially convoluted Gaussian; or (3) the exact moments of the experimental band profiles. Comparisons of the results of these methods show that the first method is always inaccurate because all the band profiles recorded are strongly tailing. The peak fit method is accurate only for 4.6 mm I.D. columns operated with instruments having low extra-column volume but fails for short narrow-bore columns due to the severe tailing of peaks passing through the complex channels of the extra-column volumes and to the inaccuracies in the fit of experimental data to the selected function. Although far better, the moment method may be inaccurate when the zero dead volume union used to measure the extra-column peak variances has a higher permeability than the column, causing the upstream part of the instrument to operate under comparatively low pressures.

1. Introduction

Recent progress in column technology, due to the advent of the shell particles that provide an unprecedented level of efficiency (>300,000 plates per meter with 4.6 mm I.D. columns [1–6]), is causing unexpected and serious challenges to the manufacturers and users of the most modern columns. First, the full performance of these new columns cannot be achieved when they are operated on standard HPLC systems (maximum pressure 400 bar), due to the excessive band broadening contributions of the upstream (injection needle, needle seat capillary, injection valve, connecting tubes) and downstream (connection tubes, detector cell) channels of these instruments. Modifications of these channels become necessary to reduce these extra-column contributions [7]. Second, the impact of the nature of the instrument used on the column performance is so critical that the manufacturers and users are often in conflict regarding the true efficiency of these columns. Quality control tests of commercialized columns are now often made with instruments modified to provide small extra-column band broadening. Most users, however, are not equipped with such modified HPLC systems and may not even understand the nature of the problem. They often find plate counts far smaller than those claimed by manufacturers. Finally, manufacturers and users could agree if there were an objective and accurate way to correct the efficiency data measured for the contributions due to extra-column band broadening. Such a correction is especially required for short narrow-bore columns (i.e., the 2.1 mm × 50 mm columns) packed with either sub-2 μm fully porous particles [8,9] or with the new core-shell particles [10,11]. Several methods have been proposed and it is necessary to assess their relative value.

The general rate model of chromatography demonstrates that, under linear conditions, the different contributions to the moments of a band are additive. The column efficiency being directly related to the values of the band moment, the determination of the correct HETP requires four separate measurements, those of the first and second moments of the peaks recorded in the presence and in the absence of the chromatographic column [12–14]. Three methods are commonly used to estimate these moments: (1) The peak apex and its half-height width can be used for this purpose; they are automatically provided by all chromatographic softwares. This method is obviously inaccurate because peak profiles are always asymmetric, particularly when the column is removed from the instrument [15,16]. Unfortunately, it is precise, simple and easy. (2) The data points of experimental peak profiles can be fitted to a mathematical peak function that is chosen as accounting for the peak tailing observed [14]. The first and the second moments are then computed from the suitable integrals of these mathematical objects. A residual error is expected because no such fit can ever

* Corresponding author. Tel.: +1 865 974 0733; fax: +1 865 974 2667.
E-mail address: guiochon@utk.edu (G. Guiochon).

0021-9673/$ – see front matter © 2011 Elsevier B.V. All rights reserved.
doi:10.1016/j.chroma.2011.05.035

be perfect but this error is neglected. (3) The four moments are calculated through the numerical integration of the experimental peak profiles. Whereas the first two approaches are necessarily approximate, the third one provides the true peak variances that are the peak characteristics needed to determine the true column HETP. In practice, when the extra-column contributions are negligible (e.g. with conventional 4.6 mm × 200 mm columns, packed with particles larger than 5 μm, and operated on instruments that were modern at the turn of the century) and the peaks nearly Gaussian, the first approach gives reasonably correct HETP data. Today, however, the extra-column contributions of these instruments are much larger than the contributions of narrow-bore, short columns (2.1 mm × 50 mm), packed with sub-2 μm fully porous particles or sub-3 μm superficially porous particles. So, serious precautions are necessary to properly assess the moments of the extra-column and the total peak profiles.

In this work, we investigate and compare the accuracy of the three methods of determination of the true column contribution to the peak variances and of the corrected plate heights of very efficient chromatographic columns. We consider two different configurations (standard and optimized) of the most modern instrument available for very high pressure liquid chromatography (VHPLC), the 1290 Infinity HPLC system, and columns of two different diameters (narrow-bore and 4.6 mm I.D.), packed with 2.7 μm core-shell Poroshell120 particles. Finally, we discuss the true efficiency of the narrow-bore Poroshell120 column for non-retained and retained compounds.

2. Theory

2.1. Column peak variance

The increase in band width caused by the sole passage of a sample zone along a chromatographic column can be derived from the increment of the zone variance between the entrance and the exit of the column. Under isocratic conditions, this contribution, $\sigma^2_{v,col.}$, to the total peak variance observed is written in volume unit square as [7]:

$$\sigma^2_{v,col.} = \frac{V_0^2}{N}(1+k)^2 \quad (1)$$

where V_0 is the column hold-up volume, N its efficiency, and k the retention factor of the sample. This expression demonstrates how important will be the role played by the extra-column contributions when the column volume is small, the column efficiency high, and the components considered poorly retained.

2.2. Instrument peak variance

Band broadening also occurs in the different parts of the HPLC system, including its injection and detection components. The complex peak variance, $\sigma^2_{v,sys.}$, results from axial dispersion along the channel followed by the sample plug, made of a series of connecting tubes with their nooks and crannies. This behavior is difficult to model accurately. An empirical model based on the coupling between axial dispersion in the stream flowing along a straight tube and radial diffusion through a side cavity was proposed to account for dispersion in these channels [17]. Yet, the effect of stagnant zones of eluent located at the connections between different parts of the system seems impossible to model accurately enough and should be determined experimentally. These dead volumes are particularly nefarious in gradient elution as they contribute significantly to increase the time necessary to re-equilibrate the column between two consecutive injections.

2.3. Total peak variance

The total peak variance measured, σ^2_{Total}, is the sum of the column and system contributions. Therefore,

$$\sigma^2_{v,total} = \sigma^2_{v,col.} + \sigma^2_{v,sys.} \quad (2)$$

In this work, we measured $\sigma^2_{v,total}$ (in the presence of the chromatographic column) and $\sigma^2_{v,sys.}$ (in the presence of a ZDV union connector which replaces the column). We discuss the different contributions of the extra-column volume to the apparent column efficiency.

3. Experimental

3.1. Chemicals

The mobile phase was a mixture of water and acetonitrile (30/70, v/v). These two solvents were HPLC grade from Fisher Scientific (Fair Lawn, NJ, USA). The mobile phase was filtered before use on a surfactant-free cellulose acetate filter membrane, 0.2 μm pore size (Suwannee, GA, USA). The samples uracil and naphthalene were purchased from Aldrich (Milwaukee, WI, USA). Each sample component was diluted in the mobile phase mixture.

3.2. Columns

The 2.7 μm Poroshell120-C_{18} columns (150 mm × 4.6 mm and 50 mm × 2.1 mm) were a generous gift from the column manufacturer (Agilent technologies, New Castle, DE, USA). The hold-up volumes of these two columns were estimated from the elution volumes of uracil corrected for the extra-column contribution and extrapolated to a flow rate equal to zero, giving 1211 and 87 μL, respectively. The total porosities of these columns are then equal to 0.49 and 0.50, respectively. The extrapolation to a zero flow rate is necessary in order to correct for the 0.05 s delay (asynchronisation time) between the moment when the zero time is recorded and the moment when the injection valve is actuated. The small total porosities of the columns result from the presence of the 1.7 μm solid non-porous core and the large average mesopore size (120 Å) of the Poroshell120 particles.

3.3. HPLC system

All the data were acquired with an Agilent 1290 Infinity HPLC system (Agilent Technology, Waldbronn, Germany) liquid chromatograph. This instrument includes a binary pump with solvent selection valves, an auto-sampler with a 20 μL sample loop, a small volume needle seat capillary (1.2 μL), a column thermostat, and a Chemstation data software. Two different configurations of this system were studied. First, the standard system configuration, including a 350 mm × 115 μm inlet capillary tube (upstream the column), a 1.6 μL active heat exchanger, a 250 mm × 85 μm outlet capillary (downstream the column), and a diode-array UV-detector (with a 2.4 μL illuminated volume). Second, the optimized system configuration includes a 250 mm × 80 μm inlet capillary tube, a 250 mm × 80 μm outlet capillary tube, and a diode-array UV-detector (with a 0.8 μL illuminated volume). Note that the heat exchanger was deliberately by-passed in this second configuration. The signal sampling rate was fixed at 160 Hz for the measurement of all extra-column band profiles. It was set at 80 and 40 Hz when the 50 mm × 2.1 mm and 150 mm × 4.6 mm columns, respectively, were installed in the oven of the instrument. Each recorded profile includes at least 60 data points or 15 data points per standard deviation σ. More than 15 data points per σ does not result in

any variation of the peak variance measured by the full integration method (see later).

The flow rate accuracy was checked at ambient temperature by directly collecting the mobile phase in the absence of column at 295 K and at flow rates of 0.1 mL/min, 1 mL/min, and 5.0 mL/min during 50, 25, and 10 min, respectively. The relative errors were all less than 0.3%, so we estimate the long-term accuracy of the flow-rate at 3 μL/min or better at flow rates around 1 mL/min. The laboratory temperature was controlled by an air conditioning system set at 295 K. The daily variation of the ambient temperature never exceeded ±1 °C.

3.4. Sample preparation and injection volumes

Two distinct vials (vial 1: uracil, vial 2: naphthalene) were prepared. First, 1 mg of uracil was dissolved in 10 mL of water at room temperature. The first vial (total volume mL) was prepared by pipetting 540 μL of the uracil water solution and adding 1260 μL of pure acetonitrile. Second, 4.3 mg of naphthalene were dissolved in 10 mL of pure acetonitrile. A second vial was prepared by pipetting 1260 μL of the naphthalene acetonitrile solution and adding 540 μL of pure water.

The sample vial concentrations were then successively diluted by a factor 1/2 until the maximum absorption signal of the peak apex recorded (4.8 μL injection, detection wavelength 254 nm) was smaller than 1500 mAU at a flow rate of 0.1 mL/min. After three successive dilutions, the final injected concentrations were 37 and 375 μg/L for uracil and naphthalene, respectively. The lowest signal-to-noise ratio was measured with the 4.6 mm I.D. column, for naphthalene, using the 2.4 μL flow cell and the 115 μm connectors, and at a flow rate of 0.10 mL/min. It is equal to 2500 and allows a very accurate measurement of the peak moments.

Volumes of 1.0 μL and 4.8 μL of these samples were injected into the 50 mm × 2.1 mm and the 150 mm × 4.6 mm 2.7 μm Poroshell120 columns in order to keep constant the sample loading per unit of column cross-section area.

3.5. Measurement of the HETP data

The peak responses were recorded at a wavelength of 254 nm for both uracil and naphthalene. The detector bandwidth was fixed at 4 nm.

The sequence of flow rates was 0.021, 0.042, 0.063, 0.083, 0.125, 0.167, 0.208, 0.250, 0.292, 0.333, 0.375, 0.417, 0.479, 0.542, 0.604, and 0.667 with the 2.1 mm I.D. column. It was 0.10, 0.20, 0.30, 0.40, 0.60, 0.80, 1.00, 1.20, 1.40, 1.60, 1.80, 2.00, 2.30, 2.60, 2.90, and 3.20 mL/min with the 4.6 mm I.D. column. Note that the sequence of linear velocity is kept the same with both columns.

For each of these 32 flow rates and for each sample, the extra-column contributions to the retention volume and to the band broadening of probes were measured by replacing the chromatographic column with a ZDV union connector.

The experimental HETP data measured for the columns were corrected for the contribution of the 1290 Infinity HPLC system. The extra-column and the total band variances were measured according to the three different approaches listed earlier. For the sake of brevity, they are called in later as (1) the half-height peak width method, (2) the peak fit method, and (3) the numerical integration method. Prior to any measurement, each profile recorded was cut on the left and the right side of the peak and corrected for baseline drift.

1. The half-height peak width method

   In this method, the retention time of the peak apex, t_R, and the half-height peak width, $w_{1/2}$, are systematically measured. The first and second central moments are derived assuming a Gaussian peak shape by:

$$\mu_1^{(1)} = t_R \tag{3}$$

$$\mu'^{(1)}_2 = \frac{w_{1/2}^2}{5.545} \tag{4}$$

2. The peak fit method

   In this method, the experimental data points of each peak were fitted to the best EMG/GMG function written, using the Seasolve PeakFit v.4.12 program, as:

$$y(t) = \frac{a_0 \ \exp(-(1/2)((a_4 t - a_1 a_4 + a_3^2)^2/a_4^2(a_3^2 + a_2^2)))[1 + \mathrm{erf}(a_3(-a_2^2 + a_4 t - a_1 a_4)/\sqrt{2}a_2\sqrt{a_3^2 + a_2^2})]}{\sqrt{2\pi}\sqrt{a_3^2 + a_2^2}\ \ \mathrm{erf}((\sqrt{2}a_3/2a_4) - 1)} \tag{5}$$

   where a_0 is the peak area, a_1 the center, and a_3 and a_4 are distortion parameters of the EMG/GMG hybrid function. Once the parameters a_0, a_1, a_2, a_3, and a_4 have been determined by multi linear regression analysis, the first and second central moments, μ_1 and μ'_2, are directed computed from the mathematical expression of the hybrid function Eq. (5):

$$\mu_1^{(2)} = \frac{\int_0^\infty y(t)t dt}{\int_0^\infty y(t) dt} \tag{6}$$

$$\mu'^{(2)}_2 = \frac{\int_0^\infty y(t)(t - \mu_1^{(2)})^2 dt}{\int_0^\infty y(t) dt} \tag{7}$$

3. The numerical integration method

   In this method, the same data points (t_i, C_i) as those used in the peak fit method were considered and the true first and second central moments were calculated as follows:

$$\mu_1^{(3)} = \frac{\sum_{i=1}^{i=N-1}(C_i + C_{i+1})((t_i + t_{i+1})/2)}{\sum_{i=1}^{i=N-1} C_i + C_{i+1}} \tag{8}$$

$$\mu'^{(3)}_2 = \frac{\sum_{i=1}^{i=N\,1}(C_i + C_{i+1})(((t_i + t_{i+1})/2) - \mu_1^{(3)})^2}{\sum_{i=1}^{i=N-1} C_i + C_{i+1}} \tag{9}$$

The moments are calculated based on the decomposition of the peak area into a series of elementary trapezes, which is more accurate than using the rectangle approach. However, if the number of points is large enough (>90), both approaches give the very same results within 0.001%.

For each method (i), the corrected reduced HETP, $h^{(i)}$, was given by:

$$h^{(i)} = \frac{L}{d_p}\frac{\mu'^{(i)}_2 - \mu'^{(i)}_{2,ex}}{(\mu_1^{(i)} - \mu_{1,ex}^{(i)})^2} \tag{10}$$

where L is the column length, d_p is the mean particle size, and $\mu_{1,ex}$ and $\mu'_{2,ex}$ are the first and second central moments of the extra-column band profiles.

Assuming the same random relative errors in presence and in absence of chromatographic errors ($\Delta\mu'_{1,ex}/\mu'_{1,ex} = \Delta\mu'_1/\mu'_1$ and $\Delta\mu'_{2,ex}/\mu'_{2,ex} = \Delta\mu'_2/\mu'_2$), the precision of the h data is given by:

$$\left|\frac{\Delta h}{h}\right| = \left|\frac{\Delta\mu'_2}{\mu'_2}\right|\left(\frac{\mu'_2 + \mu'_{2,ex}}{\mu'_2 - \mu'_{2,ex}}\right) + 2\left|\frac{\Delta\mu_1}{\mu_1}\right|\left(\frac{\mu_1 + \mu_{1,ex}}{\mu_1 - \mu_{1,ex}}\right) \tag{11}$$

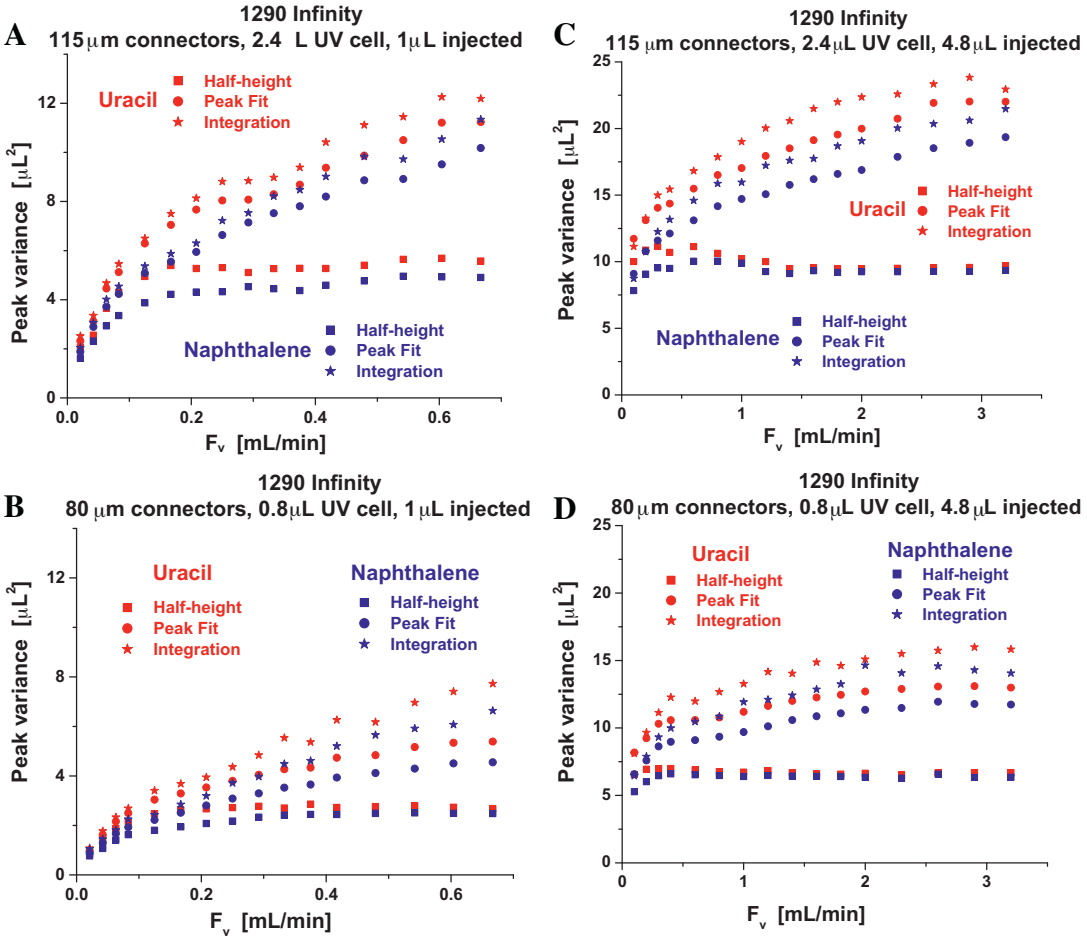

Fig. 1. Plots of the variance of the extra-column band profiles (in the absence of the chromatographic column, replaced with a ZDV union connector) of two low molecular weight compounds measured with three different methods as indicated in the legends and described in Section 3.5. Two different configurations of the instrument and two different injected volumes were considered. Standard system configuration (A and C); optimized system configuration (B and D).

The second and first moments of the peak, μ'_2 and μ_1, were measured successively three times, first with the chromatographic column, then with a zero-volume connector fitted to the instrument. The relative errors made on these moments were always less than 3 and 0.5%, for the second and the first moments, respectively. Note that the repeatability of the injection system of the 1290 Infinity HPLC system is excellent. The precision of the integration methods (2) and (3) depends essentially on the left and right cut-off abscissa. The precision of 3% was obtained when these abscissa were strictly identical at a constant flow rate. However, from one flow rate to another, the cut-off abscissa necessarily changes, therefore, the error made on the peak variance plotted as a function of the flow rate may appear larger. The relative error measured over a large range of flow rates is then larger than that measured at constant flow rate. Note that the half-height peak width method (1) dissociates itself from methods (2) and (3) because it is hardly sensitive to the position of the cut-off points.

Accordingly, if the extra-column contributions were negligible, the largest random error would be of the order of 4%, which is typically the case with large volume columns. Also, it is noteworthy that this random error necessarily increases with decreasing solute retention e.g., when the terms in between parentheses in the right-hand-side term of Eq. (11) become significantly larger than one. This contribution affects particularly small columns and/or poorly retained compounds. For instance, if μ'_2 is only twice $\mu'_{2,ex}$ and μ_1 about ten times $\mu_{1,ex}$, the maximum random error becomes close to 10%.

The relative error, $E^{(i)}$, made on the plate height data given by the half-height peak width method, $H^{(1)}$, and the peak fit method, $H^{(2)}$, were determined relative to the plate height measured by the numerical integration method, $H^{(3)}$:

$$E^{(i)} = \frac{H^{(3)} - H^{(i)}}{H^{(i)}} \tag{12}$$

4. Results and discussion

We analyze and compare the accuracy of the different methods of measurement of the second central moment (variance) of the extra-column band profiles, and those of the variance of the chromatographic columns. Then, we determine the accuracy of the half-height peak width and of peak fit methods relatively to the true value of the column HETP measured with the numerical integration method. Finally, we discuss the validity of the assumption made regarding the additivity of the variances of the extra-column and the column contributions.

4.1. Extra-column peak variances

The determination of accurate extra-column peak variance has attracted serious attention since the emergence of sub-2 μm fully porous particles and sub-3 μm superficially porous particles [7,11]. Indeed, the band broadening contribution of these instruments, even the most modern ones, remains comparable to that caused by

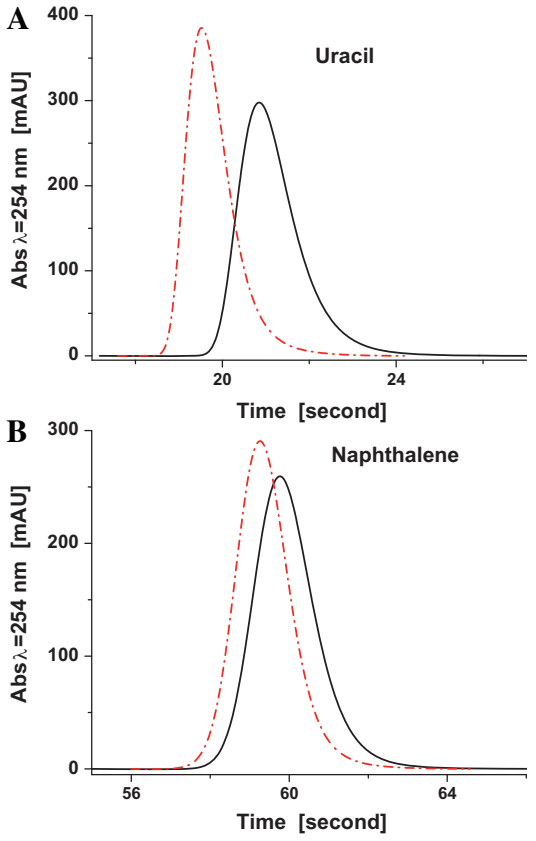

Fig. 2. Evidence of the improvement of the performance of the 2.1 mm × 50 mm column after minimization (dash dotted line) of the extra-column volume of the standard configuration (solid line) of the instrument. Flow rate: 0.292 mL/mL. (A) Compound: non-retained uracil ($k = 0$). (B) Compound: retained naphthalene ($k = 2.2$). In addition to the reduction in the peak width, note the decrease of the elution time by about 1.5 s.

the most efficient chromatographic columns. Extra-column band broadening results from the axial dispersion of the sample along the different parts of the instruments. The presence of a parabolic flow profile across tubes and of stagnant zones of eluent explains why extra-column peak profiles are significantly distorted [15]. The extent of this peak deformation depends on the system configuration, the volume of sample injected, the eluent linear velocity, and the sample diffusion coefficient (i.e., sample mass, solvent viscosity, temperature, and pressure). Accordingly, extra-column peak profiles should be recorded for a given compound, a given eluent, and a fixed temperature.

4.1.1. System configurations

Two different system configurations were studied (see Section 3 for details). Fig. 1A and B compares the extra-column variance contributions measured for the 2.1 mm i.d. column with a 1.0 μL size sample for uracil (red symbols) and naphthalene (blue symbols), with the standard and the optimized configurations, respectively. Fig. 1C and D do the same for the 4.6 mm i.d. column with a 4.8 μL sample size. Interestingly, shrinking the inner diameter of the two connecting tubes from 115 to 80 μm and the UV detection cell volume from 2.4 to 0.8 μL and bypassing the 1.6 μL heat exchanger of the instrument leads to a relative decrease of the variance of about 40%. This explains the obvious decrease of the peak width obtained for the narrow-bore column seen in Fig. 2A (uracil, $k = 0$) and B (naphthalene, $k = 2.2$) which compare the peak profiles recorded with the two system configurations at the same flow rate of 0.292 mL/min.

4.1.2. Injection volumes

In order to inject the same mass of sample per unit of column cross-section area, 1.0 and 4.8 μL samples were injected into the 2.1 and the 4.6 mm I.D. columns, respectively. The comparison between Fig. 1A and C, on the one hand, between Fig. 1B and D, on the other, shows a relative decrease of the extra-column variance contributions close to 50%. Had the injection profile been an ideal rectangular plug at the exit of the injection needle, the contributions to this variance would be 0.08 and 1.92 μL^2, e.g. a difference of only +1.84 μL^2. In fact, this difference was measured at ca. +8 μL^2 independently of the system configuration. Axial dispersion certainly takes place during the drawing and the ejection of the sample in and from the sample loop (20 μL). New injection methods have been designed to cut the tail of the sample zone before it reaches the needle seat capillary of HPLC instruments [18]. This could markedly decrease the extent of band broadening before the band enters the column.

4.1.3. Nature of the sample compound

We used two different compounds, uracil and naphthalene. The former is practically unretained on silica-C_{18} stationary phases while the latter has a retention factor of the order of 2 with a 30/70 (v/v) mixture of water and acetonitrile as the eluent. Fig. 1A through D compare the extra-column peak variances of uracil (red star symbols) and naphthalene (blue star symbols). Interestingly, the peak variance of uracil is systematically 17% larger than that of naphthalene. According to the Wilke and Chang correlation [19], the diffusion coefficients of uracil and naphthalene in this acetonitrile/water solution are 1.44 and 1.11 × 10^{-5} cm^2/s. The profiles of the peaks of these two compounds exhibit practically the same front but the tailing of the uracil peak is slightly more pronounced. This would appear at first to be inconsistent with the faster relaxation of concentration gradients across the connecting tubes. Most likely, this is due to the presence of dead volumes (such as cracks or anfractuosities at the connections between different parts of the instrument) along the channel. Compounds with a large diffusion coefficient move deeper and in larger amount into side cavities when the sharp front of the peak passes but take longer to diffuse out because the driving force, the concentration gradient, decreases along the peak tail. This could explain the longer tail of the injection profile of uracil.

Most importantly, this result illustrates why the extra-column volume contributions of each compound should be measured separately.

4.1.4. Linear velocity

At high eluent linear velocity, the injected compound does not have enough time to sample the whole cross-section of the connecting tubes. Therefore, peak distortion is essentially controlled by the parabolic flow profile of the mobile phase across these tubes. Molecules moving in the center of the tubes elute first (front of the peak) whereas molecules located close to the tube walls are eluted last (peak tailing). In contrast, at low flow rates (but if band broadening is not controlled by longitudinal diffusion), there is enough time for the analyte to sample most of the tube diameter. According to Aris theory of dispersion in cylindrical tubes [20], the asymptotic limit for the ratio of the variance increment, $d\sigma^2$, to the time increment, dt, is

$$\lim_{t\to\infty} \frac{d\sigma^2}{dt} = \frac{1}{96}\frac{D_c^2 U^2}{D_m} \quad (13)$$

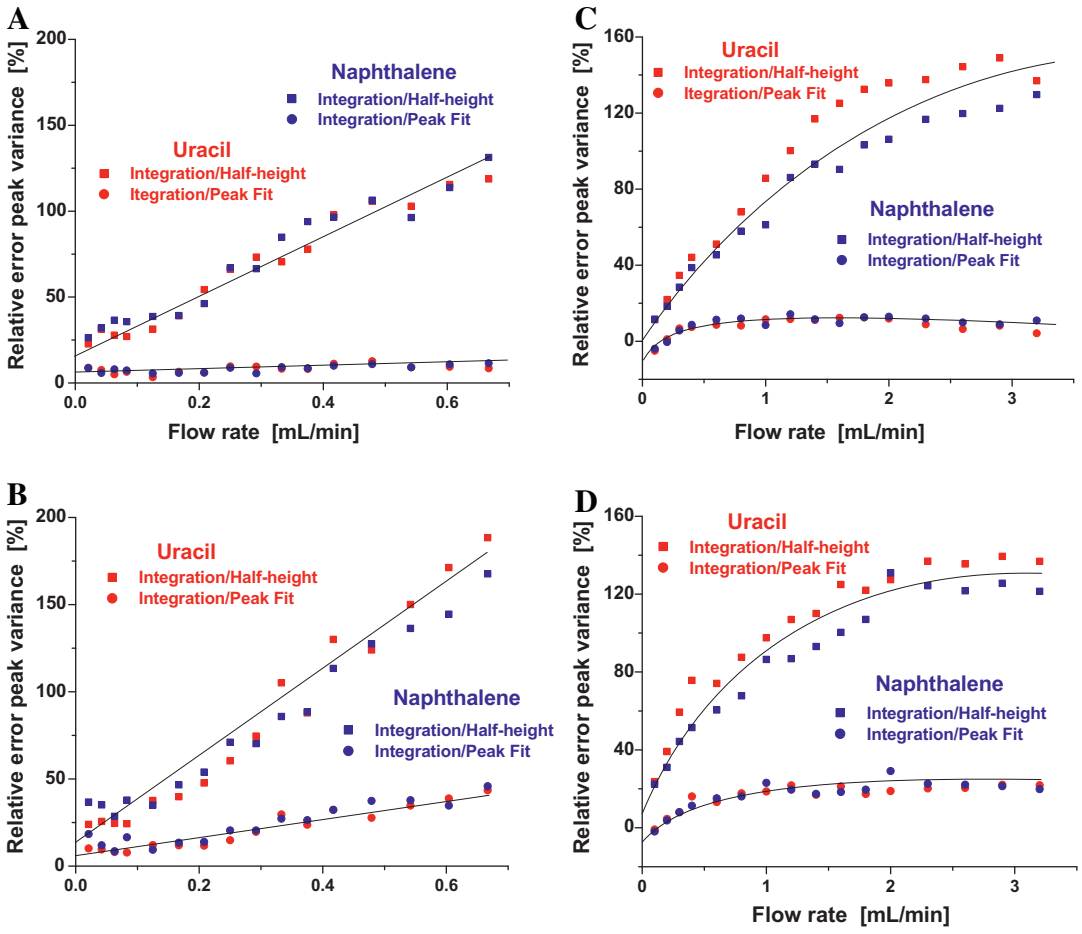

Fig. 3. Plots of the relative difference between the peak variances measured by the numerical integration method and the half-height peak width method (full square symbols), on one hand, and the peak fit method (full circle symbols), on the other hand. Same system configurations (A–D) as in Fig. 1.

where D_c is the tube diameter, U is the linear velocity ($U = F_v/\pi R_c^2$), and D_m the diffusion coefficient. Since $dz = Udt$, after integration from $z = 0$ to $z = L$

$$\frac{1}{D_c}\frac{\sigma^2(z=L)}{L} = \frac{1}{96}\frac{UD_c}{D_m} \quad \text{or} \quad h_c = \frac{1}{96}\nu_c \tag{14}$$

Accordingly, if the extra-column channels in the equipment were empty tubes, the plot of the reduced plate height, h_c, versus the reduced linear velocity, ν_c, would be linear with a slope of 1/96, since axial dispersion is controlled by the radial diffusion of the sample. These plots (not shown) were constructed for uracil and naphthalene, for flow rates between 0.021 and 0.667 mL/min. They are not linear but convex upward. Extrapolation of the ratio h_c/ν_c at zero flow rate (or $t \to \infty$) gives slopes of about 0.10, a value one order of magnitude larger than expected. Thus, a pure diffusion process does not control axial dispersion along these channels.

In conclusion, the effect of the linear velocity of the eluent on the extra-column variance contribution is non-linear. Peak variances reach an upper limit at high velocities, beyond 2.5 and 3.0 mL/min with 80 μm and 115 μm connecting tube diameters, respectively. From a chromatographic point of view, this translates into an increase of the peak asymmetry with increasing flow rate because, as the flow rate increases, diffusion has less and less time to relax the radial concentration gradients of sample components across the extra-column volume connections. Again, these results are consistent with the model of irregular channels with multiple side cavities in which molecules are trapped and may escape only by diffusion. Compounds with large diffusion coefficients move deeper and in larger amounts into side cavities and it takes longer for them to exit because the driving force, the concentration gradient, is far steeper when they enter these cavities than when they escape.

4.1.5. Accuracy of the measurements

To further achieve the purpose of this work, we compare the accuracy of the measurements of the extra-column variance contributions made with the half-height peak width and the peak fit methods. Obviously, the systematic tailing of peaks eluted through the extra-column volumes makes the first method clearly inappropriate to assess the true value of the variance contribution of the instrument. Fig. 3A through D shows the relative errors made with the two approximate methods, compared with the result of numerical integration of the experimental data. As the peak asymmetry, the relative error increases with increasing flow rate. This error is the same for both compounds. Remarkably, the true peak variance can be 1.5 to twice larger than the result of the half-height peak width method, which should never be considered to estimate true column HETP when the extra-column contributions are significant. In contrast, the peak fit method gives a relative error that increases with decreasing connector diameter. The true peak variance is on the average 10 and 20% larger than those measured by the peak fit method with capillaries of 115 and 80 μm i.d., respectively. The origin of this error stems from the relatively poor quality of the fit of the rear part of the experimental data to the EMG/GMG hybrid function, when the sample concentration tends toward zero. Accordingly, the peak fit method is acceptable at low flow rate (see Fig. 3B) when the peak asymmetry remains moderate but it should be rejected at high flow rates.

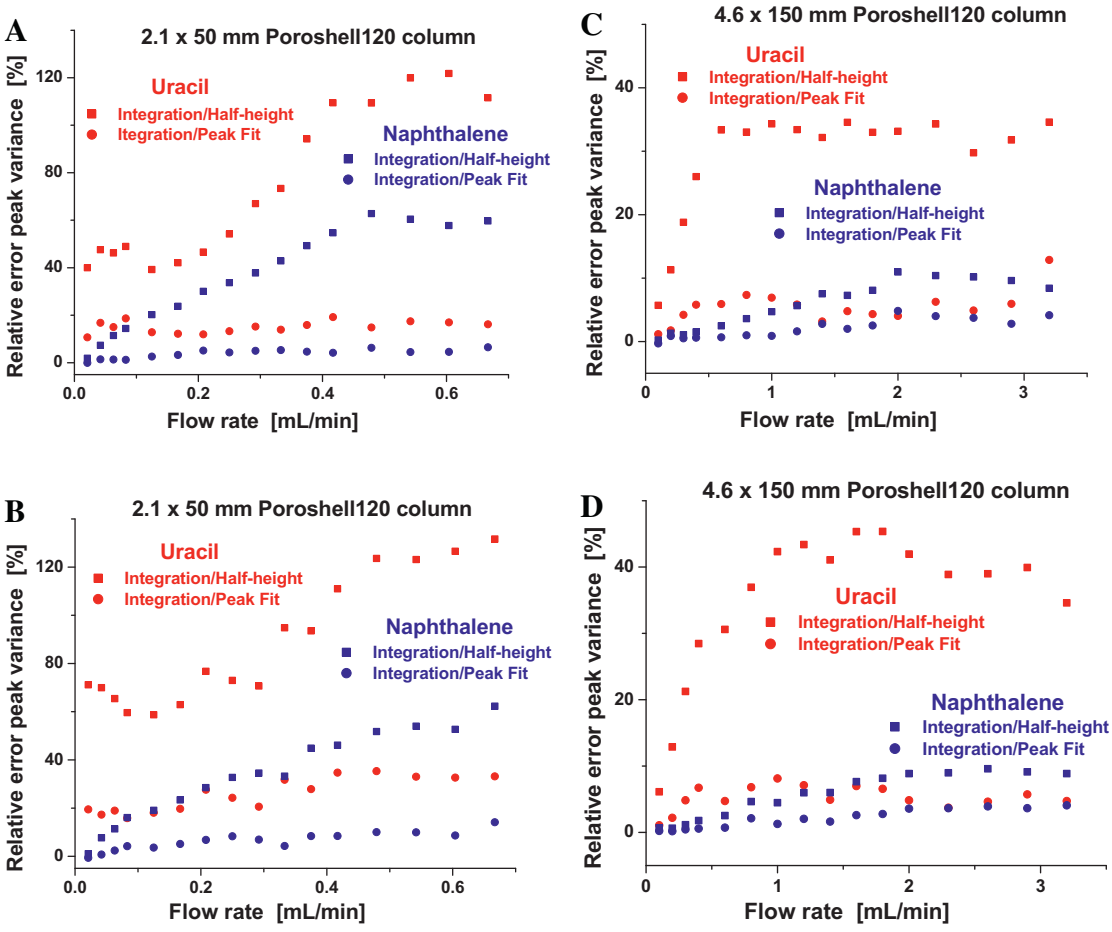

Fig. 4. Plots of the relative difference between the total peak variances measured from the numerical integration method and the half-height peak width method (full square symbols), on one hand, and the peak fit method (full circle symbols), on the other hand. Same system configurations (A–D) as in Fig. 1.

In conclusion, the measurement of the variances of the peaks eluted through the extra-column volumes and the ZDV depends much on the method used. Unambiguously, nor the half-height peak width nor the peak fit methods are suitable for this purpose. Only the exact numerical integration of the peak profiles should be considered.

4.2. Total peak variances

The total peak variances were also measured for the two Poroshell120 columns. Eq. (1) shows that this variance increases with increasing retention factor k and hold-up volume V_0. These variances were measured for the peaks of uracil ($k = 0$) and naphthalene ($k = 2.2$) on the two columns ($V_0 = 0.09$ and 1.21 mL). With the standard configuration of the instrument, the extra-column contribution barely affects the peak variance of the most retained compound on the larger column (this contribution represents less than 5% of the variance due to the column). In contrast, the extra-column contribution represents up to 20% for the variance due to the column for the non-retained compound, uracil. Most importantly, the extra-column contribution to band broadening accounts for up to 30 and 40% of the total peak variance of naphthalene and uracil, respectively, with the narrow-bore column.

Even for the determination of the total peak variance, the accuracy of the half-height peak width method is insufficient because all the peaks observed are not symmetrical. The peak fit method is suitable with the 4.6 mm I.D. column because the peak tailing remains moderate and can be well described by the EMG/GMG hybrid function. However, only the numerical integration should be considered for measurements made with the narrow bore column. Fig. 4A–D shows the plots of the relative error made when using the half-height peak width and the peak fit methods. They confirm the importance of the errors caused by the use of these approximative methods, 20% (peak fit) to 100% (half-height peak width) with narrow-bore, short columns and non-retained compounds. These errors decrease to 7 and 40% with the 4.6 mm I.D. column. If we consider a compound with a moderate retention factor of 2.2, these relative errors decrease to 10 and 50% (2.1 mm I.D. column) and 3 and 10% (4.6 mm I.D. column).

Overall, for the sake of accuracy in measurements of column plate height, only the numerical integration method should be used to measure the total peak variances.

4.3. Reduced HETP plots

We determined the corrected reduced plate heights of uracil and naphthalene on both columns, using the two system configurations, according to the three methods described in Section 3.5. The results are shown in Fig. 5A–D. The calculations show that the peak fit method provides nearly (within a few percent) the same plate heights values of naphthalene with both columns. Given the accuracy of the data (Section 3.5), the peak fit and the numerical integration methods are found to be equivalent for the measurement of the plate heights of retained compounds. In contrast, this method generates errors of 5–30% with the 4.6 mm I.D. and the narrow-bore columns, respectively, for the non-retained compound, uracil. Note that the half-height peak width method grossly underestimates the true plate height of naphthalene, by

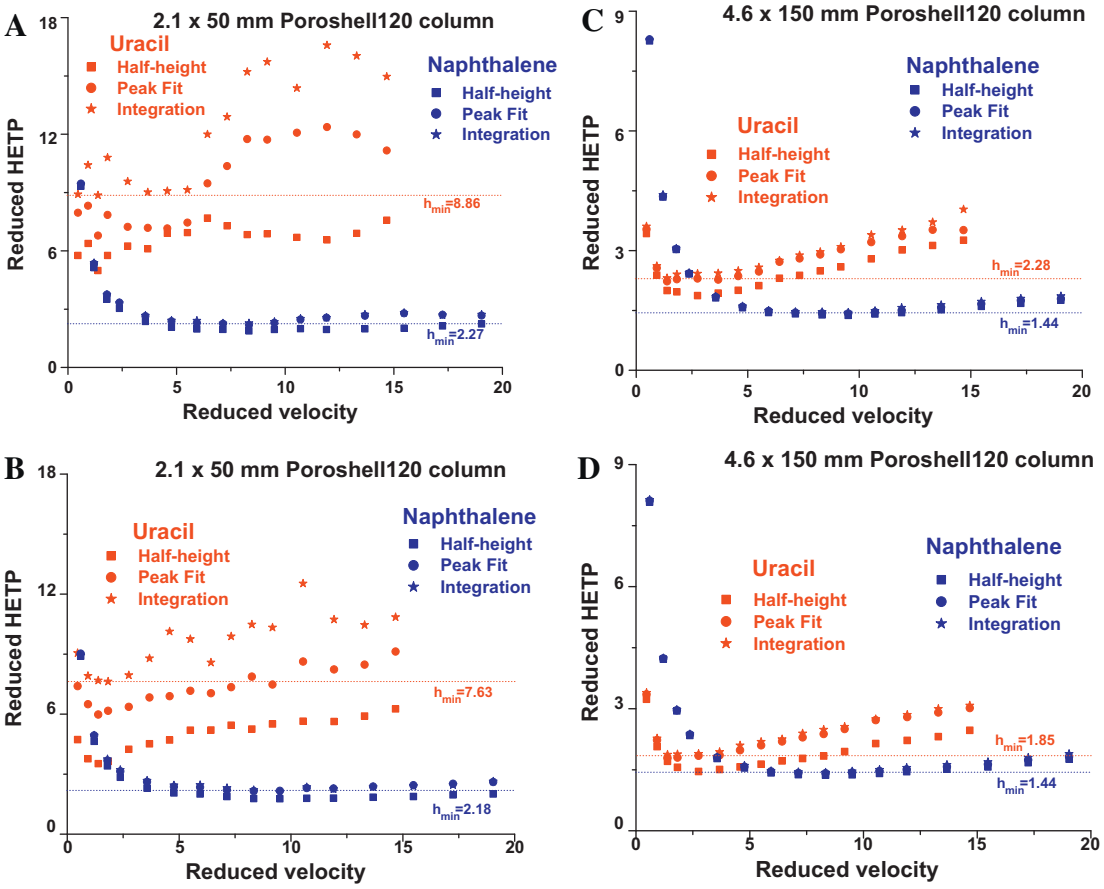

Fig. 5. Plots of the corrected reduced HETP of two small molecules measured from three different methods as indicated in the legend and described in Section 3.5. Same system configurations (A–D) as in Fig. 1.

−7% and −30% with the 4.6 mm I.D. and the narrow-bore columns, respectively. Again, as expected, these relative errors increase to −30 and −50% for the non-retained compound, uracil. The good agreement between the peak fit and the numerical integration methods for retained compounds is explained by the large peak variance of these compounds and their nearly symmetrical peak shape.

However, in many cases (poorly retained compounds and narrow-bore columns), significant errors are generated unless the numerical integration method is used in the determination of the plate heights. Although the half-height peak width and the peak fit methods provide more robust results (the level of the noise of the plate height data of uracil increases from the half-height peak width to the peak fit to the numerical integration method, see Fig. 5A and B), their accuracy remains poor because they do not properly take into account the contribution of the rear tailing of the uracil peak profile.

4.4. Additivity of the peak variance

In this section, we discuss the validity of the additivity of the peak variance that was postulated earlier, by comparing the corrected reduced plate height plots of uracil and naphthalene versus the reduced velocity measured with two different instrument configurations. Fig. 6A and B shows the results obtained for the true peak variances (numerical integration).

It is interesting that the two configurations of the instrument provide corrected reduced plate heights that are nearly identical for the retained naphthalene (average relative difference of 1 and 5% for the 4.6 and 2.1 mm I.D. columns, respectively), whereas a significant difference is measured with the non-retained uracil (average relative difference of 18% for both columns). The optimized configuration of the instrument (80 μm capillaries with a 0.8 μL UV cell) gives systematically smaller reduced plate heights.

In conclusion, the two different configurations of the instrument give the same systematic relative difference (+18%) between the corrected plate heights of uracil for the 4.6 mm × 150 mm Poroshell120 column. This difference is significant even though the extra-column variance contribution accounts for 20% (115 μm capillaries) and 17% (80 μm capillaries) of the total peak variance of uracil. The maximum random error of measurements in this case is about 6%, clearly smaller than the systematic difference of 18% observed. In theory, peak variance additivity applies and the same corrected plate height should be observed and there is no *a priori* reason to doubt that it does. We must conclude that the zero dead volume (ZDV) union connector used does not permit an accurate measurement of the extra-column band broadening contribution. This is because the ZDV union does not offer a pressure resistance comparable to that of chromatographic columns. It was not feasible to find and use a ZDV having that high flow resistance. A longer capillary restrictor might provide the same permeability as the column but, due to its volume, it would contribute to a larger extent to the extra-column band broadening. This would bias the measurement.

Most importantly, these results show that using the same chromatographic column and the same method of measurement does not guarantee that the same corrected column efficiency will be obtained. The same instrument configuration must be used. It is highly probable that two instruments of the same model, which might have been modified differently over time to the extent that it is possible will provide different extra-column variance con-

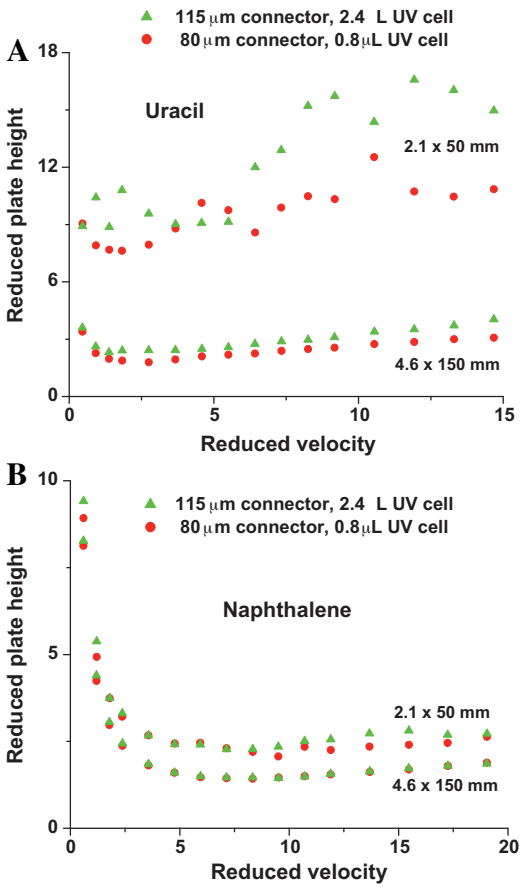

Fig. 6. Plots of the corrected reduced HETP of uracil (A) and naphthalene (B) measured from the numerical integration method and from two different contributions of the 1290 infinity system. Note the nearly undistinguishable HETP of the retained compound, naphthalene.

tributions. Also, the extra-column variance contribution depends on the mobile phase composition and on the sample component used, through its diffusion coefficient. This explains why serious disagreement are frequently observed between the level of efficiency found by column manufacturer and by users or by different users (possibly in the same group). The column efficiencies are measured with different equipments and phase systems, which differ markedly in performance.

4.5. Performance of the Poroshell120 columns

We have used in this work the most accurate method available to us. Our results show that the intrinsic (or corrected) plate heights of the Poroshell120 columns depend strongly on the column diameter. The minimum reduced plate height of the moderately retained, nonpolar naphthalene is 1.4 and 2.2 for the 4.6 and the 2.1 mm I.D. columns, respectively. The minimum reduced plate heights of the non-retained uracil are 1.8 and 7.6 for the same columns. This illustrates and confirms the major problem that all column manufacturers are currently facing: how could it be possible to pack superficially porous particles in narrow-bore and in conventional 4.6 mm I.D. tubes and obtain columns having the same efficiency [10,11]? The analysis of the reduced HETP curves in Fig. 6B suggests that the reduced eddy diffusion term is larger in 2.1 than in 4.6 mm I.D. column by nearly 1 h unit. This cannot be explained by a difference in the trans-channel velocity biases, the impact of which on the reduced HETP is less than 0.3 h unit. Also, according to recent simulation studies [21,22], packed beds having the same external porosity (0.40) have similar eddy diffusion term, with small differences in the order of the packed bed ($\Delta h < 0.2$). Therefore, differences in the short-range inter-channel velocity biases cannot be responsible for the difference in these HETP curves either.

Most likely, 4.6 mm I.D. columns are more radially homogeneous than 2.1 mm I.D. columns. The nefarious wall effects seem to be worse in 2.1 mm I.D. column while they seem to barely affect the packing structure in the central region of 4.6 mm I.D. columns. This would be consistent with the decrease of the corrected column efficiency observed when the retention factor decreases and tends toward zero [23] (Fig. 6A). Nonretained molecules have less time during their elution to diffuse radially and relax the radial concentration gradients caused by the trans-column velocity biases [23].

5. Conclusion

Our results confirm that serious systematic errors are made when approximate methods are used to measure peak moments (centroid and variance). Clearly, the half-height peak width method provides gross underestimates and cannot be used to determine the true plate height of any compound on narrow-bore columns nor that of weakly retained compounds on 4.6 mm I.D. columns. Because the performance of sub-3 μm core-shell particles is comparable to that of sub-2 μm fully porous particles, the measurement of the accurate corrected plate height of such columns requires the use of better methods that properly account for the asymmetry of chromatographic peaks. Despite the fact that modern instruments have low extra-column volumes, the profiles of bands eluted through ZDV connectors remain strongly unsymmetrical. Fitting the experimental peak profiles to a mathematical function accounting for this tailing and extracting its first and second moments provides a better solution. Yet, even a complex function containing up to 5 independent parameters cannot perfectly account for actual peak shapes. This peak fitting method fails to predict true corrected plate heights of narrow-bore columns, even though it provides accurate values for broader columns (with errors less than 1 and 5% for retained and nonretained compounds, respectively). Most importantly, our results demonstrate that one cannot determine the true corrected plate height of narrow-bore columns unless the exact numerical integration of the actual elution profile is performed.

This result is of great importance when narrow-bore columns must be tested in several laboratories or their true performance must be assessed. The performance of different columns cannot be compared unless they are measured with the same instrument. The use of different instruments is a common source of disagreement between manufacturers and users. True column efficiency depends not only on the experimental conditions selected but also on the method used for the calculation of the band moments. The true moments should always be measured by numerical integration after baseline correction with small I.D. columns.

Finally, the comparison between the corrected reduced plate heights of a non-retained compound measured for two different configurations of our 1290 Infinity HPLC system show systematic difference because, despite the exactness of the integration method, extra-column variances measured with a ZDV union connector slightly differ from the actual extra-column variance contributions that take place in the presence of a column. This small difference has nearly no consequence, however, regarding the determination of the true corrected HETP of retained compounds.

Acknowledgements

This work was supported in part by grant CHE-06-08659 of the National Science Foundation and by the cooperative agreement

between the University of Tennessee and the Oak Ridge National Laboratory. We thank Ron Majors (Agilent Technologies, New Castle, DE, USA) for the generous gifts of the Poroshell120 column used in this work and for fruitful discussions.

References

[1] F. Gritti, G. Guiochon, J. Chromatogr. A 1157 (2007) 289.
[2] J.J. DeStefano, T.J. Langlois, J.J. Kirkland, J. Chromatogr. Sci. 46 (2008) 254.
[3] S.A. Schuster, B.M. Wagner, B.E. Boyes, J.J. Kirkland, J. Chromatogr. Sci. 48 (2010) 566.
[4] F. Gritti, I. Leonardis, D. Shock, P. Stevenson, A. Shalliker, G. Guiochon, J. Chromatogr. A 1217 (2010) 1589.
[5] F. Gritti, G. Guiochon, J. Chromatogr. A 1217 (2010) 1604.
[6] F. Gritti, I. Leonardis, J. Abia, G. Guiochon, J. Chromatogr. A 1217 (2010) 3219.
[7] C. Gritti, F. Sanchez, T. Farkas, G. Guiochon, J. Chromatogr. A 1217 (2010) 3000.
[8] F. Gritti, G. Guiochon, J. Chromatogr. A 1216 (2009) 1353.
[9] F. Gritti, G. Guiochon, J. Chromatogr. A 1217 (2010) 1485.
[10] F. Gritti, G. Guiochon, J. Chromatogr. A 1217 (2010) 5069.
[11] E. Olah, S. Fekete, J. Fekete, K. Ganzler, J. Chromatogr. A 1217 (2010) 3642.
[12] J. Sternberg, J.C. In, R.A. Giddings, Keller (Eds.), Advances in Chromatography, vol. 2, Marcel Dekker, New York, NY, 1966.
[13] J. Kirkland, W. Yau, H. Stoklosa, C.H. Dilks, J. Chromatogr. Sci. 15 (1977) 303.
[14] G. Guiochon, A. Felinger, A. Katti, D. Shirazi, Fundamentals of Preparaative and Nonlinear Chromatography, 2nd ed., Academic Press, Boston, MA, 2006.
[15] J.G. Atwood, M.J.E. Golay, J. Chromatogr. 218 (1981) 97.
[16] J.G. Golay, M.J.E. Atwood, J. Chromatogr. 186 (1979) 353.
[17] K.J. Fountain, U.D. Neue, E.S. Grumbach, D.M. Diehl, G. Guiochon, J. Chromatogr. A 1216 (2010) 5979.
[18] J. Samuelsson, T. Fornstedt, Anal. Chem. 80 (2008) 7887.
[19] C. Wilke, P. Chang, Correlation of diffusion coefficients in dilute solutions, AIChE J. 1 (1955) 264.
[20] R. Aris, Proc. R. Soc. A 235 (1956) 67.
[21] A. Daneyko, A. Holtzel, S. Khirevivh, Anal. Chem. 83 (2011) 3903.
[22] S. Khirevich, A. Daneyko, A. Holtzel, A. Seidel-Morgenstern, U. Tallarek, J. Chromatogr. A 1217 (2010) 4713.
[23] F. Gritti, G. Guiochon, J. Chromatogr. A 1217 (2010) 6350.